

## Analysis of Range Extension Process for Outdated Ballistic Munitions Ejected from an Accelerator Launcher Concept

Ceyhun TOLA<sup>1\*</sup> , Pınar BEYAZPINAR<sup>2</sup> , Deniz AKIN<sup>2</sup> 

<sup>1</sup> Aselsan Inc, Microelectronics, Guidance & Electro-Optics Division, Ankara, Turkey

<sup>2</sup> University of Turkish Aeronautical Association, Department of Astronautical Engineering, Ankara, Turkey

### Abstract

In this study, the feasibility of a new launcher concept that provides range extension for outdated ballistic munitions by speeding up them before their ignition is examined in detail. To analyze the efficiency of the new concept, multi-variable and single-variable optimization processes are conducted using the Multi-Objective Genetic Algorithm Method in the ModeFrontier environment. Launch angle, ejection velocity of the munition from the launcher, and ignition delay of the rocket motor after the ejection process are determined as design variables. An in-house MATLAB script is prepared and validated to perform numerical solutions of the munition's two-dimensional trajectory. As a result of the optimization processes, graphical results are prepared to examine the effects of each design variable on munition's range and to make a comparison between the flight trajectories of the munitions which are launched from classical and accelerator launchers. It is concluded that usage of the accelerator launcher concept provides approximately 20% range extension for the generic munition examined in this research when compared to the classical launcher. Since this new concept can easily be adapted to different types of outdated ballistic munitions and the cost of the accelerator launcher development process will probably less than the cost required to develop new munitions, it will be reasonable to develop accelerator launchers such as electromagnetic accelerators or catapult launchers in near future.

**Keywords:** Range Optimization, Accelerator Launcher Concept, 2-D Trajectory Solver, ModeFrontier

### 1. Introduction

Today, advanced military systems such as fighters, unmanned aerial vehicles, and rockets/missiles have been developed by many countries to ensure their security. Such systems are used for both defensive and offensive purposes. During military operations, the range of a munition

has crucial importance since long-range systems provide an opportunity to attack under less amount of risk when compared with short-range systems. Therefore, different improvement and optimization studies on range improvement have been conducted so far. While some studies focused on trajectory

**Corresponding Author:** Ceyhun Tola [ceyhuntola@gmail.com](mailto:ceyhuntola@gmail.com)

**Citation:** Tola C., Beyazpinar P., Akin D. (2021). Analysis of Range Extension Process for Outdated Ballistic Munitions Ejected from an Accelerator Launcher Concept J. Aviat. 5 (2), 90-100.

**ORCID:** <sup>1</sup> <https://orcid.org/0000-0001-9056-0543>; <sup>2</sup> <https://orcid.org/0000-0003-0495-9393>; <sup>3</sup> <https://orcid.org/0000-0001-9264-7060>

**DOI:** <https://doi.org/10.30518/jav.974811>

**Received:** 27 July 2021 **Accepted:** 17 November 2021 **Published (Online):** 20 December 2021

**Copyright © 2021 Journal of Aviation** <https://javsci.com> - <http://dergipark.gov.tr/jav>



This is an open access article distributed under the terms of the Creative Commons Attribution 4.0 International Licence

optimization, some of them focused on aerodynamic shape optimization and propulsion system concept optimization.

Yang et al. optimized the range of a canard-controlled missile by optimizing its aerodynamic shape benefiting from the genetic algorithm method [1]. Tanrikulu and Ercan offered an optimal external configuration design method to optimize the range, stability, and warhead performance of missiles [2]. Li et al. performed a multiphase trajectory optimization process to optimize the downrange of a boost-glide missile [3]. Dilan, preferred the Genetic Algorithm Method in order to optimize trajectory optimization of a tactical missile [4]. Vasile et al. conducted an aerodynamic design optimization of control surfaces for a long-range projectile using the particle swarm optimization method [5]. Pue et al. performed a multidisciplinary concept optimization of a ballistic missile [6]. Şumnu et al. used the Multi-objective Genetic Algorithm to optimize the aerodynamic shape of a missile in order to determine the optimum lift and drag coefficients [7].

Technological improvements in defense systems push designers to improve the capability of the munitions in use since the improvement of already developed systems is generally much cheaper than the development of new munitions. For example, it is possible to improve the hitting accuracy of the air to ground classical munitions by modifying them with laser-guided kits such technology has been used to modify the classical MK-82 bombs in Turkey. Similarly, with the technological improvements, it will be possible to extend the range of outdated ballistic munitions with the assistance of special launcher concepts such as catapult systems or electromagnetic launchers in near future. Those launchers will provide an initial ejection velocity to the munitions during launch to further extend their range. For instance, it will be possible to provide a range extension for classical ballistic munitions such as TR-107 or TR-122 rockets which are widely used by the Turkish Army.

In literature, different studies on electromagnetic guns have been conducted so far. The majority of them focus on the development or optimization of a coilgun concept to accelerate a bullet or a projectile using electromagnetic rails [8-10]. Some studies focus on the aerodynamic analysis of hypersonic projectile geometries launched from

electromagnetic launchers [11]. Neither of the studies in literature aims to extend the range of the classical ballistic munitions benefiting from electromagnetic launchers. This research will be the first one that analyzes the feasibility of accelerator concept on range maximization of ballistic munitions. To analyze the feasibility of this new concept, multivariable and single variable optimization processes are conducted.

During the range improvement, it is quite significant to determine the sensitivity of launch parameters on munition's range. After the munition is ejected from the launcher, it will be ignited in a very short time. Therefore, besides the launch angle ( $\theta$ ), two more parameters those are ejection velocity of the munition from the launcher ( $V_0$ ) and ignition delay after the ejection from the launcher ( $t_{fire}$ ) will gain importance during the development of new generation launcher systems and during the range optimization of the munitions.

Within the content of this work, range optimization of a generic ballistic munition that is ejected from an accelerator launcher is performed. Launch angle ( $\theta$ ), ejection velocity of the munition from the launcher ( $V_0$ ), and ignition delay after the ejection from the launcher ( $t_{fire}$ ) are selected as design variables (optimization parameters) to maximize the munition's range. Results of the multivariable optimization process are used to make a comparison between the results of the classical munition launch process. Additionally, independent single variable optimization processes are conducted and graphical results are prepared in order to examine the effects of each design variable on munition's optimum range. Numerical solution of the problem is performed using an in-house MATLAB script. Optimization processes are prepared and conducted in ModeFrontier software.

## 2. Methodology

This part aims to summarize the basic mathematical model to solve the 2-D trajectory motion of the ignited generic munition just after it is ejected from the accelerator launcher. The solution of the trajectory can be divided into three different phases:

- Phase 1: Coasting (Before Ignition)
- Phase 2: Powered Flight
- Phase 3: Coasting (After Burnout)

In the first phase, the munition is ejected from the launcher with an initial  $V_0$  velocity and it performs short coasting until the munition's solid rocket motor is ignited. With the ignition of the solid rocket motor, the second phase of the flight (powered flight) is started and this phase ends up whenever the solid rocket motor burns out. Then, a second coasting phase which corresponds to "Phase 3" starts and lasts until the munition hits the ground. All of the flight phases are illustrated in Figure 1.

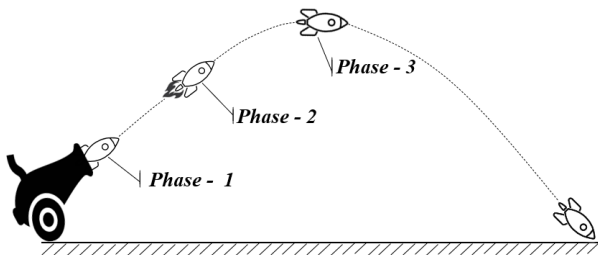


**Figure 1.** Flight phases of the munition ejected from accelerator launcher concept

The two-dimensional, flight trajectory of the munition can be calculated by applying Newton's second law to each of the flight phases for both of the x and y directions. Throughout the solutions, it is assumed that the aerodynamic lift force generated by the munition is negligible.

**2.1. Phase-1: Costing Before Ignition**

During Phase-1, since the munition is not ignited, the mass of the system is constant and equal to the total mass of the munition. There is not any thrust or lift force, but gravitational and aerodynamic drag forces are present as shown in Figure 2. Using Figure 2 and applying Newton's Second Law in x and y directions, Equations 1 and 2 can be written sequentially.

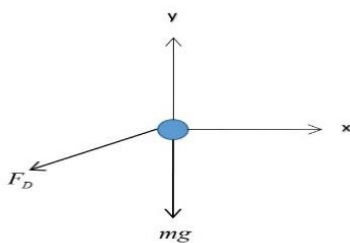


**Figure 2.** Free body diagram of munition for Phase-1 and Phase-3

$$-F_D \cos(\theta) = m\ddot{x} \tag{1}$$

$$-mg - F_D \sin(\theta) = m\ddot{y} \tag{2}$$

where  $\theta$  represents the launch angle,  $g$  corresponds to gravitational acceleration,  $m$  represents the instant mass of the munition, and  $F_D$  corresponds to the instant drag force.  $x$  and  $y$  symbolize accelerations corresponding to x and y axes.

The drag force depends on the velocity of the munition ( $v$ ), the density of air ( $\rho_{air}$ ), drag coefficient ( $C_D$ ), and reference area ( $A_f$ ) of the munition. It can be calculated using Equation 3.

$$F_D = C_D A_f \rho_{air} \frac{v^2}{2} \tag{3}$$

Since the altitude of the munition is variable with time, the density of the air is also variable. Using the altitude information, the density of the air is calculated with Equation 4.

$$\rho_{air} = \rho_0 \cdot e^{-h/h_{scale}} \tag{4}$$

where  $\rho_0$  defines sea-level density of the air (1.225 kg/m<sup>3</sup>),  $h$  and  $h_{scale}$  correspond to the altitude and density scale height (7500 m) sequentially.

The drag coefficient is another variable in Equation 3. It varies with the velocity of the munition and it depends on the shape of the munition. In some studies, the drag coefficient is assumed as constant; but, within the content of this work it is taken as variable, and variation of the drag coefficient with Mach number is illustrated in Figure 3.

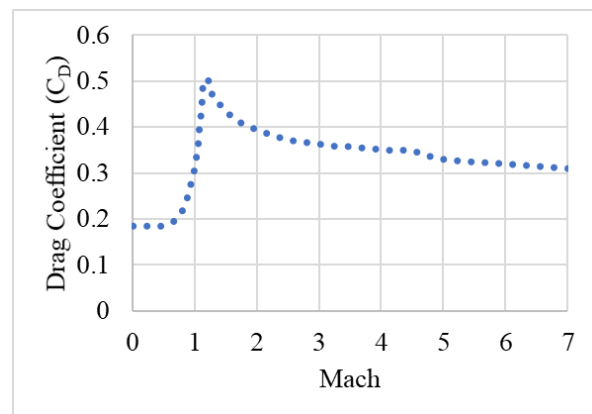


**Figure 3.** Variation of drag coefficient with Mach

Similar to the air density, gravitational acceleration also varies with altitude. Using the altitude information, it can be calculated as in Equation 5.

$$g = \frac{g_0}{1 + (h/R_e)^2} \tag{5}$$

where  $g_0$  defines gravitational constant at sea level (9.8066 m/s<sup>2</sup>),  $R_e$  represents the radius of the Earth (6378 km), and  $h$  is the altitude.

The munition velocity ( $v$ ) can be calculated using Equation 6.

$$v = \sqrt{\dot{x}^2 + \dot{y}^2} \quad (6)$$

where  $\dot{x}$  and  $\dot{y}$  define velocities in x and y directions. They can also be stated in Equations 7 and 8.

$$\dot{x} = v \cos(\theta) \quad (7)$$

$$\dot{y} = v \sin(\theta) \quad (8)$$

Thus, Equations 9 and 10 can be derived.

$$\cos(\theta) = \frac{\dot{x}}{v} = \frac{\dot{x}}{\sqrt{\dot{x}^2 + \dot{y}^2}} \quad (9)$$

$$\sin(\theta) = \frac{\dot{y}}{v} = \frac{\dot{y}}{\sqrt{\dot{x}^2 + \dot{y}^2}} \quad (10)$$

Finally, using Equations 1, 2, 3, 9, and 10; Equations 11, 12, 13, and 14 can be derived.

$$\ddot{x} = -\frac{C_D A_f \rho_{air} v^2}{2m} \cos(\theta) \quad (11)$$

$$\ddot{x} = -\frac{C_D A_f \rho_{air}}{2m} \dot{x} \sqrt{\dot{x}^2 + \dot{y}^2} \quad (12)$$

$$\ddot{y} = \frac{-mg - F_D \sin(\theta)}{m} \quad (13)$$

$$\ddot{y} = -g - \frac{C_D A_f \rho_{air}}{2m} \dot{y} \sqrt{\dot{x}^2 + \dot{y}^2} \quad (14)$$

where  $m$  corresponds to total mass of the munition that is equal to  $m_0$ .

Numerical solution of Equations 12 and 14 with respect to time is accomplished using a Runge-Kutta solver prepared in MATLAB environment. Thus, the trajectory solution of the first phase is completed.

### 2.2. Phase-2: Powered Flight

During Phase-2, since there is an ignition process, the thrust force is also added to the free body diagram as shown in Figure 4. On the other hand, the mass of the munition is decreasing with time due to the propellant burning process. Using Figure 4 and applying Newton's Second Law in x

and y directions, Equations 1, and 2 are updated as Equations 15, and 16.

$$(F_T - F_D) \cos(\theta) = m\ddot{x} \quad (15)$$

$$(F_T - F_D) \sin(\theta) - mg = m\ddot{y} \quad (16)$$

where  $F_T$  defines the thrust force.

Within the content of this study, it is assumed that the munition's solid rocket motor produces a constant (7500 N) trust during the powered flight phase.

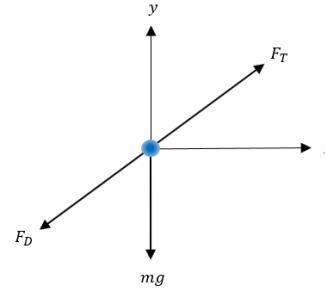


**Figure 4.** Free body diagram of munition for Phase-2

On the other hand, the mass of the munition is decreasing during the powered flight and it can be calculated using Equation 17.

$$m(t) = m_0 - \dot{m} \cdot t \quad (17)$$

where  $t$  defines time and  $\dot{m}$  defines propellant mass flow rate.

Assuming that the propellant mass flow rate is constant, the mass flow rate can be calculated using Equation 18.

$$\dot{m} = \frac{F_T}{I_{sp} \cdot g_0} \quad (18)$$

where  $I_{sp}$  represents the specific impulse of the solid rocket motor, and  $g_0$  corresponds to the gravitational constant at sea level.

Applying a similar solution procedure with Phase-1 and using Equations 3, 9, 10, 15, and 16; Equations 19, 20, 21, and 22 are derived.

$$\ddot{x} = \frac{1}{m} \left( F_t - \frac{C_D A_f \rho_{air} v^2}{2} \right) \cos(\theta) \quad (19)$$

$$\ddot{x} = \frac{\dot{x}}{m \cdot \sqrt{\dot{x}^2 + \dot{y}^2}} \cdot \left( F_t - \frac{C_D A_f \rho_{air} v^2}{2} \right) \quad (20)$$

$$\ddot{y} = \frac{(F_T - \frac{C_D A_f \rho_{air} v^2}{2}) \sin(\theta)}{m} - g \quad (21)$$

$$\ddot{y} = \frac{\dot{x} \cdot (F_T - \frac{C_D A_f \rho_{air} v^2}{2})}{m \cdot \sqrt{\dot{x}^2 + \dot{y}^2}} - g \quad (22)$$

The numerical solution of Equations 20 and 22 with respect to time is accomplished using the Runge-Kutta solver.

**2.3. Phase-3: Coasting After Burnout**

During Phase-3, since the propellant is burned out, there is not any thrust force exerted on the system. Additionally, the mass of the munition is constant and equal to the final mass (final mass = total mass – propellant mass). The free-body diagram of this last phase is identical with Phase 1 and it was illustrated in Figure 2. The only difference between Phase 1 and Phase 3 is the mass of the munition. Thus, after placing the final mass ( $m_f$ ) into Equations 12, and 14; then solving it with the Runge-Kutta solver, the trajectory solution of the last phase is finalized.

**3. Validation**

An in-house MATLAB script is prepared to perform the numerical solution expressed in the previous section.

Since the accelerator-type launcher concept is quite new, it is not possible to find out an experimental result covering a real rocket launch process from a catapult or from an electromagnetic launcher. Therefore, in order to validate the numerical solution procedure, experimental results presented in Nathan’s study are used [12]. In that research, the trajectory of a spinning and non-spinning baseball is examined by conducting experiments [12]. Spinning baseball produces lift force due to Magnus Effect [12]. Since the munition’s aerodynamic lift force is neglected in this study, experimental results belonging to the non-spinning baseball trajectory of Nathan’s research are used to validate our numerical model. Properties of the baseball used for validation are listed in Table 1.

The drag coefficient of the ball varies with respect to velocity and this property is taken from Adair’s book [13]. Figure 5 illustrates the variation of baseball’s drag coefficient with velocity.

After the data is digitized and a suitable unit conversion process is accomplished, the in-house MATLAB script developed within the content of

this research is updated in accordance with the experimental inputs in Nathan’s study [12].

**Table 1.** Properties of baseball [12]

Property	Value	Unit
Mass	0.145	kg
Diameter	0.0728	m
Initial velocity	44.704	m/s
Launch angle	30	deg
Initial vertical location	0.875405	m

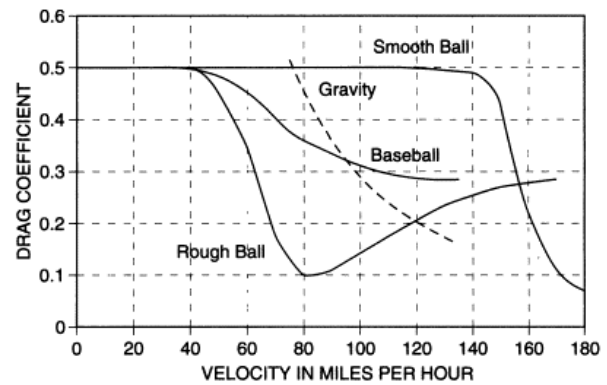


**Figure 5.** Variation of the drag coefficient [13]

Figure 6 shows the comparison of numerical results belonging to this study with Nathan’s experimental results [12].

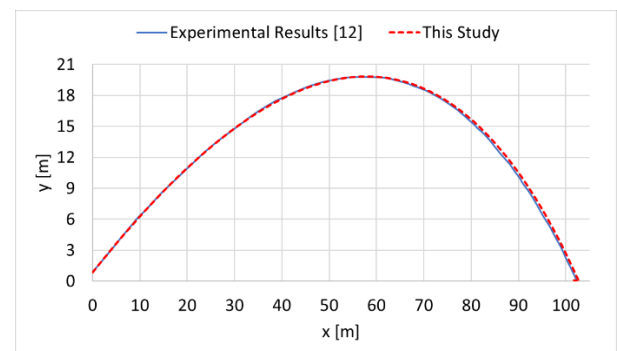


**Figure 6.** Validation of the numerical solution procedure [12]

As it can be seen from Figure 6, there is a good agreement between the experimental and numerical results. This validation process shows that the developed in-house MATLAB script performs accurate calculations for the first and final phases of the real problem. However, it is unnecessary to perform further validation process for Phase 2 since

only the mass of the munition is varying with time and there is an additional constant positive thrust force component in the numerical solution process unlike the other flight phases, and adding or subtracting a force to the equation or solving the equation using variable mass does not change the numerical solution procedure. Thus, the developed in-house MATLAB script can be used for the range optimization process.

#### 4. Range Optimization

This section aims to maximize the range of a generic munition by launching it from the accelerator launcher concept and determining the effects of design parameters on the range. Properties of the munition are listed in Table 2.

**Table 2.** Properties of the generic munition

Property	Value	Unit
Total Mass	75	kg
Final Mass	35	kg
Diameter	0.122	m
Specific Impulse	250	s
Drag Coefficient	Figure 3	-

The drag coefficient of the munition varies with respect to velocity and its behavior was illustrated in Figure 3. Before the optimization process, the maximum range of the munition and the launch properties providing the maximum range are listed in Table 3.

**Table 3.** Before the optimization process maximum range of the munition

Property	Value	Unit
Launch Angle	75.35	deg
Range	145.314	km
Flight Time	224.05	s

The optimization process is divided into two different parts. In the first part, launch angle ( $\theta$ ), ejection velocity of the munition from the accelerator launcher ( $V_0$ ), and ignition delay after

the ejection ( $t_{fire}$ ) are determined as design variables. Using MOGA-II (MultiObjective Genetic Algorithm II) solver of the ModeFrontier, munition’s range is maximized. In the second part, the effects of each design variable on munition’s range are examined separately by taking two of them as constant and one of them as a variable.

The Multiobjective Genetic Algorithm Method is an efficient optimization method that can find out the global maximum or minimum point of the problem with high accuracy since it searches diverse regions of the solution space. The method is based on mimicking the biological evolution principle. An initial population is generated and subsequent generations are constructed following the genetic algorithm operators such as the probability of directional cross-over, probability of selection, probability of mutation, and DNA string mutation ratio. Iterative generation of new populations provides conversion of the optimization problem to its optimum point.

The reason behind the selection of MOGA-II solver is due to its success in finding out the global maximum value (solver’s robustness) and its accuracy.

#### 4.1. Multi-variable Optimization

This section presents range maximization of the munition by changing three design variables listed in Table 4. The only objective of the optimization process is summarized in Equation 23.

$$\min_{s \in S} \frac{1}{Range(s)} \tag{23}$$

The upper and the lower limits of the design variables are given in Equation 24 and listed in Table 4.

$$S = \{s \in \mathbb{R} \mid s_L \leq s \leq s_U\} \tag{24}$$

$$s = \{\theta, V_0, t_{fire}\}$$

**Table 4.** Design variables and limits

Design Variable	$s_L$	$s_U$	Step	Unit
Launch Angle	35	75	0.1	deg
Ejection Velocity	60	120	0.2	m/s
Ignition Delay	0	1	0.01	s



The ejection velocity limits may seem to be high but usage of electromagnetic launchers or new generation catapult systems will provide those ejection velocities depending on both the size and mass of the munitions. Step size defines the increment or decrement step of the variable during the optimization process. For example, the launch angle can be taken as  $42.8^\circ$ ; but it cannot be taken as  $42.78^\circ$  since the step size is determined as  $0.1^\circ$ .

Workflow of the optimization process modeled in ModeFrontier environment is illustrated in Figure 7.

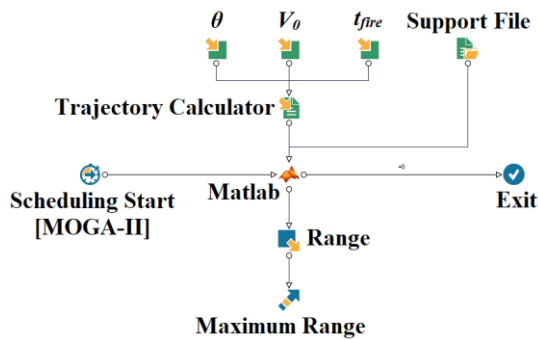


Figure 7. Multi-variable optimization workflow

As can be seen from the figure, MOGA-II scheduling node manages the optimization process. Three design variables are defined at the top and numerical solver (in house MATLAB script) is defined as “Trajectory Calculator”. Runge-Kutta solver is stored as a function; therefore, it is given to the MATLAB node as “Support File”. MATLAB node performs a solution for each design and gives the “Range” output. Then as an objective, the range is maximized.

After performing 562 runs, the optimization process is accomplished. Results of the multi-variable optimization process are illustrated in Figure 8 and 9. The graphs shown in the figure are three-dimensional. While x and y axes correspond to launch angle ( $\theta$ ), and range; colored legends correspond to ejection velocity ( $V_0$ ) and ignition delay ( $t_{fire}$ ) for Figure 8, and 9 sequentially. In the legend, blue means lower, and red means higher values for ejection velocity and ignition delay parameters.

Table 5 summarizes the optimum values of the design variables for the maximum range.

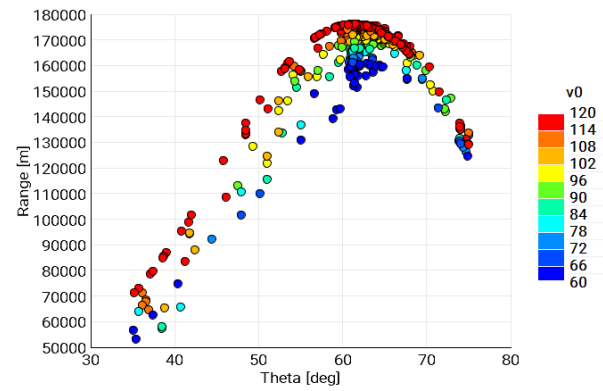


Figure 8. Variation of range with launch angle and ejection velocity

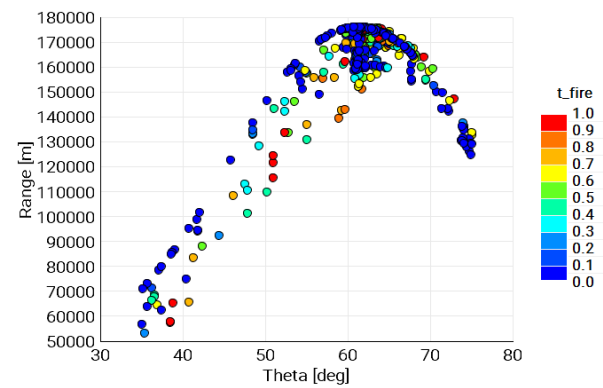


Figure 9. Variation of range with launch angle and ignition delay

Table 5. Multi-variable optimization results

Property	Value	Unit
Launch Angle	61.3	Deg
Ejection Velocity	120	m/s
Ignition Delay	0	s
Range	176.048	km
Flight Time	242.94	s

According to the optimization results, higher ejection velocity extends the range. In order to reach the farthest range, the ignition delay is set to 0 s (which means that the munition has to be immediately ignited) and the launch angle has to be set at  $61.3^\circ$ . Usage of accelerator launcher provides 21.15% range extension. The optimum launch angle that provides maximum range is decreased from  $70.35^\circ$  to  $61.3^\circ$  (12.86% decrement). On the other hand, there is 8.43% total flight time increment is

calculated with the usage of the accelerator launcher concept.

The classical (traditional) launcher is a conventional missile/rocket launcher it can store the munition inside it and arrange its launch angle. On the other hand, the accelerator (new generation) launcher also provides initial ejection velocity to the munition during the launch process in addition to the properties of the classical launcher. The accelerator launcher concept benefits from the electromagnetic rails or catapult systems to speed up the munition.

Figure 10 to 14 illustrate the comparison of trajectory simulation results belonging to both the classical and accelerator launchers.

Figure 10 presents the variation of horizontal position with vertical position (altitude) of the munition. Figure 11, and Figure 12 show the variation of horizontal and vertical positions of the munition with time sequentially. Finally, variations of horizontal and vertical velocities of the munition with time are plotted in Figure 13, and Figure 14 sequentially.

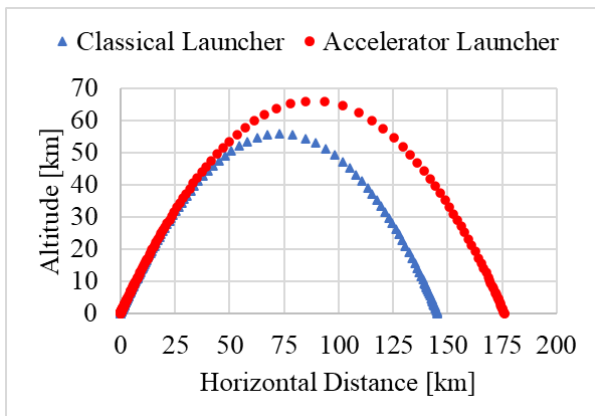


Figure 10. Horizontal position - Altitude

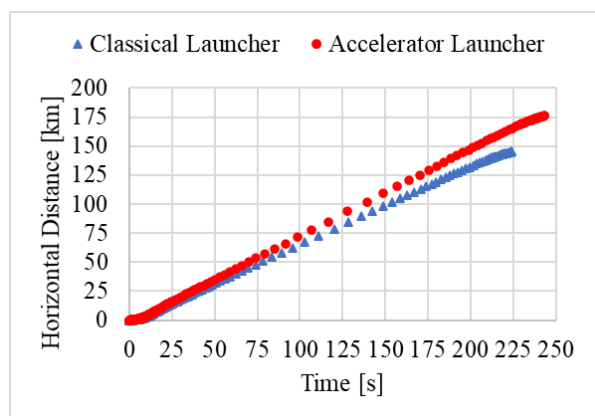


Figure 11. Horizontal position - Time

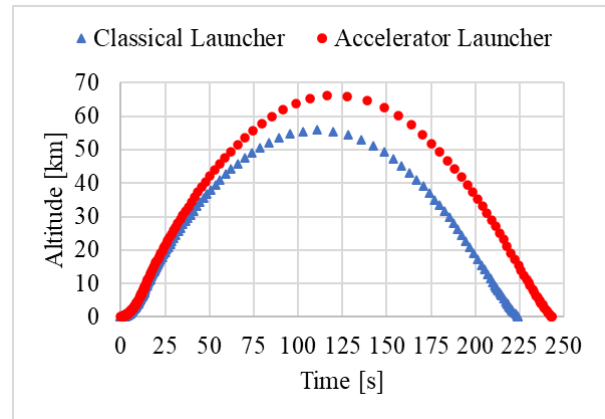


Figure 12. Altitude - Time

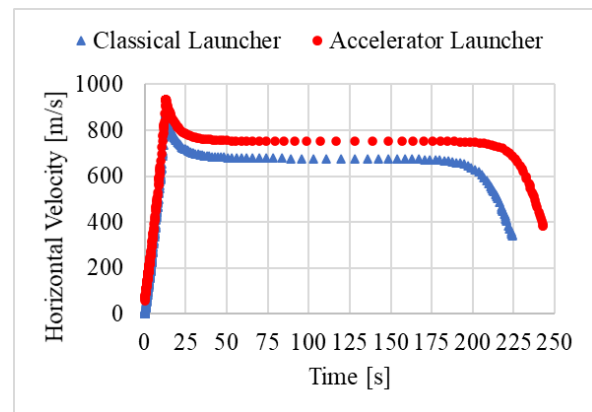


Figure 13. Horizontal velocity - Time

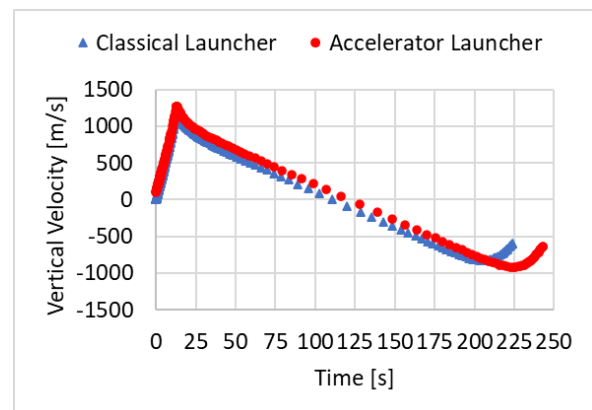


Figure 14. Vertical velocity - Time

According to the simulation results, after the ignition, there is a sudden increment in both vertical and horizontal velocity components. After the burnout, there is a sharp decrement in both of the velocity components at the vicinity of 13.08 s for both of the launch cases. The reasons for this situation are of course the drag and the gravitational forces. For the accelerated launch case at  $t=116.4$  s, the munition reaches its highest altitude that is 66040 m while for the classical launch case at  $t=110.9$  s the munition reaches its highest altitude that is 55860 m. Finally, for the accelerated launch



case, the munition hits the ground at the end of 242.94 s flight time with a vertical velocity of 640 m/s and a horizontal velocity of 383.4 m/s while for the classical launch case those values are 224.05 s, 342.3 m/s, and 595.8 m/s respectively. The range is calculated as 176.048 km for the accelerated launch case while the classical launcher provides 145.314 km range.

#### 4.2. Single Variable Optimization

In order to examine the effects of each design variable on munition’s range separately; single variable optimization processes are accomplished by taking two of them as constant and one of them as a variable. By changing constant values and repeating the optimization processes; graphical results are produced to compare the effects of differing the values of launch angle ( $\theta$ ), ejection velocity ( $V_0$ ) and, ignition delay ( $t_{fire}$ ) on optimum results.

In order to examine the effect of ignition delay on optimum launch angle results, constant ejection velocity is taken as 90 m/s, and ignition delay is changed from 0 s to 1 s with 0.25 s intervals. Figure 15 shows how the optimum launch angle is changing depending on different ignition delay parameters.

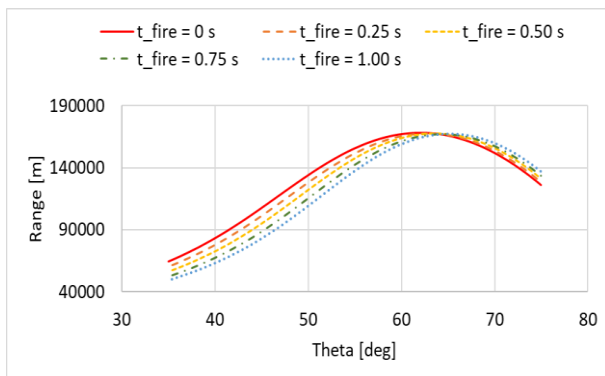


**Figure 15.** Variation of optimum Launch Angle with different Ignition Delay values

According to the results, the optimum launch angle decreases with the decrement of constant ignition delay. This can be understood from the slight shift of the curves from right to left with the decrement of the ignition delay.

In order to make a detailed result evaluation, the left and right sides of the optimum launch angle can be examined separately. In Figure 15, the left side of the optimum launch angle illustrates that the decrement of the ignition delay increases the range.

On the other hand, the right side of the optimum launch angle shows that increment of the ignition delay up to a certain threshold increases the range. If the munition is launched with low launch angles (such as 40°) without any thrust force, its nose immediately turns downward direction in less amount of time. This leads to less flight time and a shorter range. However, if the munition is launched with high launch angles (such as 70°) it takes a higher amount of time to turn down its nose in the downward direction. Thus, it is possible to extend its range by making a late ignition and so increasing its flight time. Although the horizontal velocity vector is small if the flight time is enough, the munition’s range can be further.

Similarly, in order to examine the effect of ignition delay on ejection velocity results, constant launch angle is taken as 55° and ignition delay is changed from 0 s to 1 s with 0.25 s intervals. Figure 16 shows how range is changing depending on different ignition delay and ejection velocity parameters.

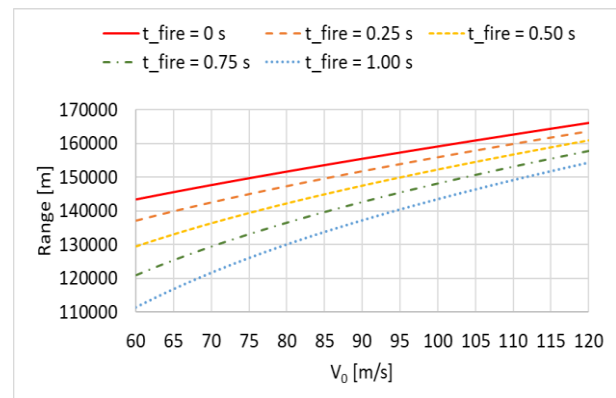


**Figure 16.** Variation of optimum Ejection Velocity with different Ignition Delay values

According to the results, the range increases with the decrement of ignition delay. Ignition delay is much more effective for the lower ejection velocities since late ignition leads to the decrement of the munition velocity too much and this requires more time to speed up the munition in higher gravitational force. Therefore, ejection velocity increment is much more effective on munition’s range for higher ignition delay.

Finally, to examine the effect of ejection velocity on optimum launch angle results, the constant ignition delay is taken as 0.5 s and ejection velocity is changed from 60 m/s to 90 m/s with 15 m/s intervals. Figure 17 shows how the optimum launch

angle is changing depending on different ejection velocity values.

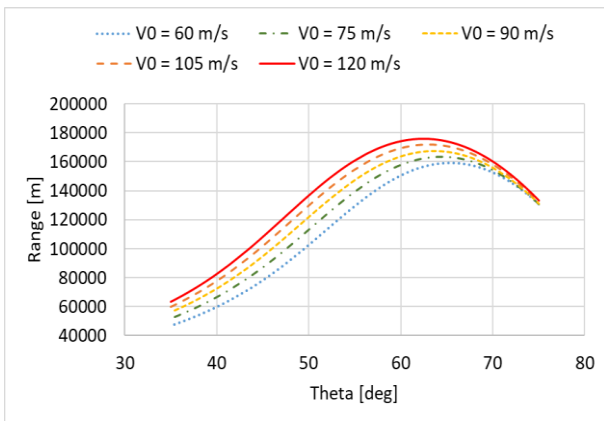


**Figure 17.** Variation of optimum Launch Angle with different Ejection Velocity values

According to the results, optimum launch angle decreases with the increment of constant ejection velocity. Since it is possible to reach higher altitudes in less amount of time with higher ejection velocities, it is possible to extend the range of the munition with less amount of launch angle. On the other hand, if the launch angle is too high (such as 75°) increment of the ejection velocity has a very small effect on the horizontal velocity component of the munition. Therefore, the distance between the ranges for higher and lower ejection velocities is quite small for very high launch angles.

### 5. Conclusion

Trajectory analysis and range optimization of a generic ballistic munition launched from an accelerator launcher concept are accomplished to analyze the feasibility of the accelerator launcher concept within the content of this work. Electromagnetic accelerator launchers and new generation catapult accelerators are examples of this concept. To simulate the trajectory, an in-house MATLAB script is prepared and validated. The optimization process is modeled in the ModeFrontier environment and during the optimization process, the Multi-Objective Genetic Algorithm II (MOGA-II) scheduler is used since it provides both robustness and accuracy. Range maximization is the only objective of the optimization process. To find out the optimum range, 3 design variables which are launch angle, ejection velocity, and ignition delay are changed in between certain intervals. Maximum range is achieved by minimizing the ignition delay,

maximizing the ejection velocity, and setting the launch angle as 61.3°.

21.15% range extension is provided with the usage of accelerator launcher concept instead of classical launcher for the generic ballistic munition examined within the context of current research. Flight time is increased by 8.43%. The optimum launch angle providing the maximum range is decreased from 70.35° to 61.3° with the usage of the accelerator launcher instead of the classical one.

To make further examination on effects of each design variable on munition’s range separately; single variable optimization processes are performed. Graphical results of this process represent several results. Decrement of the ignition delay decreases the optimum launch angle. For launch angles that are smaller than the optimum value, the range can be extended by decreasing the ignition delay. For launch angles that are higher than the optimum value, the range can be extended by increasing the ignition delay. Ignition delay is more effective on munition’s range for lower ejection velocities since late ignition leads to the decrement of the munition velocity too much and more time is needed to speed up the munition in higher gravitational force. Ejection velocity increment is much more effective up to moderate launch angles (such as 60°) when compared with higher values (such as 75°) since its increment has negligible changes in horizontal velocity components of the munition for very high launch angles. Results of this research also show that the development of accelerator launchers provides a considerable amount of range extension for classical ballistic munitions as long as their launch angle is not too high.

In conclusion, the development of accelerator launchers will make significant contributions to the range extension process of outdated ballistic munitions with low cost in near future. Results of this work give an idea about how much amount of range extension may be provided for some Turkish ballistic munitions. Considering approximately 20% range extension will be provided by the accelerator launcher concept, the range of a T-122 Sakarya rocket can be extended from 40 km to 48 km. With the technological improvements, the range extension to cost ratio will further decrease gradually.

## 6. Symbols

$\theta$ : Launch angle  
 $\rho_0$ : Sea level density of air  
 $\rho_{air}$ : Density of air  
 $A_f$ : Reference area  
 $C_D$ : Drag coefficient  
 $F_D$ : Instant drag force  
 $F_T$ : Thrust force  
 $g$ : Gravitational acceleration  
 $g_0$ : Gravitational acceleration at sea level  
 $h$ : Altitude  
 $h_{scale}$ : Density scale height  
 $I_{sp}$ : Specific impulse  
 $m$ : Instant mass of the munition  
 $m_f$ : Final mass of the munition  
 $m_0$ : Total mass of the munition  
 $\dot{m}$ : Propellant mass flow rate  
 $R_e$ : Radius of the Earth  
 $s_L$ : Lower limit of the design variables  
 $s_U$ : Upper limit of the design variables  
 $t$ : Time  
 $t_{fire}$ : Ignition delay  
 $v$ : Velocity of the munition  
 $V_0$ : Ejection velocity  
 $\dot{x}$ : Velocity in x direction  
 $\ddot{x}$ : Acceleration in x axis  
 $\dot{y}$ : Velocity in y direction  
 $\ddot{y}$ : Acceleration in y axis

### Ethical Approval

Not applicable

### References

- [1] Y. R. Yang, S. K. Jung, T. H. Cho, and R. S. Myong, "Aerodynamic shape optimization system of a canard-controlled missile using trajectory-dependent aerodynamic coefficients," *Journal of Spacecraft and Rockets*, 49, 243–249, 2012.
- [2] O. Tanrikulu, and V. Ercan, "Optimal external configuration design of unguided missiles," *Journal of Spacecraft and Rockets*, 35, 312–316, 1998.
- [3] Y. Li, N. Cui, and S. Rong, "Trajectory optimization for hypersonic boost-glide missile considering aeroheating," *Aircraft Engineering and Aerospace Technology: An International Journal*, 81, 3–13, 2009.
- [4] B. D. Özdil, "Trajectory Optimization of a Tactical Missile by using Genetic Algorithm," Middle East Technical University Graduate School of Natural and Applied Sciences, M.Sc. Thesis, 2018.
- [5] J. D. Vasile, J. T. Bryson, and F. E. Fresconi, Aerodynamic Design Optimization of Long Range Projectiles using Missile DATCOM: AIAA SciTech 2020 Forum, January 06-10, 2020, Orlando, ABD.
- [6] A. J. Pue, R. J. Hildebrand, D. E. Clemens, J. R. Gottlieb, J. M. Bielefeld, and T. C. Miller, "Missile concept optimization for ballistic missile defense," *Johns Hopkins Apl. Technical Digest*, 32, 774–786, 2014.
- [7] A. Sumnu, I. H. Guzelbey, and O. Ogucu, "Aerodynamic shape optimization of a missile using a multiobjective genetic algorithm," *International Journal of Aerospace Engineering*, 2020, 1–17, 2020.
- [8] J. Zhou, and T. Liu, "Physical analysis and optimization of electromagnetic coilgun launch systems," *American Journal of Physics*, 87, 894–900, 2019.
- [9] S. J. Lee, L. Kulinsky, B. Park, S. H. Lee, and J. H. Kim, "Design optimization of coil gun to improve muzzle velocity," *Journal of Vibroengineering*, 17, 554–561, 2015.
- [10] S. J. Lee, J. H. Kim, B. S. Song, and J. H. Kim, "Coil gun electromagnetic launcher (EML) system with multi-stage electromagnetic coils," *Journal of Magnetism*, 18, 481–486, 2013.
- [11] J. Shen, S. Fan, Y. Ji, Q. Zu, and J. Duan, "Aerodynamics analysis of a hypersonic electromagnetic gun launched projectile," *Defence Technology*, 16, 753–761, 2020.
- [12] A. M. Nathan, "The effect of spin on the flight of a baseball," *American Journal of Physics*, 76, 119–124, 2008.
- [13] R. K. Adair, *The Physics of Baseball*. New York, ABD: Perennial, 2002.